Measurement of Noise in Electronic Devices by the Fourier Transform Method

I. V. Padalka[f], 🆔 0009-0007-4071-5878

I. S. Virt[s], Dr.Sc.(Phys.-Math.) Prof., 🆔 0000-0001-7200-6055

Ivan Franko State Pedagogical University of Drohobych ℞ 04vpyax58
Drohobych, Ukraine

Abstract—The paper considers and analyzes the method of measuring the noise characteristics of electronic circuits and devices based on data collection by a digital oscilloscope with a built-in Fourier transform. The measurement process methodology and its analysis are demonstrated when determining the noise characteristics of industrial resistors. This includes, in particular, thermal (white) noise, which is the predominant type of resistor noise. The work includes an overview of the noise properties of resistors and existing measurement methods, as well as an understanding of the theory of such measurements.

To determine the sources of noise in industrial resistors, a real-time fast Fourier transform (*FFT*) of the signal was run on an oscilloscope. Thermal (white) noise spectra were determined using the *FFT* tool using a total number of 2^{12} points.. However, it is difficult to make any recommendations as to which setup should be used for a particular resistor type or technology, as for most setups the noise level is unknown and only a few measurement results are available.

The ratio of the average value of the power spectral density (*PSD*) of thermal noise in the frequency range of measurements to its calculated theoretical value based on the ohmic rating of the measuring coal industrial resistors was estimated.

Keywords — electronic devices; resistors; spectral analysis; Fourier transformation; thermal noise; noise diagnostics.

I. INTRODUCTION

These studies are aimed at developing diagnostics of electronic elements. In particular, in application to the development of resistor technologies. With the increasing demands on precision electronics, resistor noise as an additional parameter plays an important role. The selection of an appropriate resistor depends on many parameters. While all resistors exhibit unavoidable thermal noise, often referred to as Johnson noise, there is also excess noise, known as current noise. The magnitude and nature of the noise depends on the technology of manufacturing the resistor and the current flowing through it. Resistor technology and the reduction of excess noise require the development of test equipment for its determination. There are well-known standards for measuring excess noise in resistors [1], [2]. There are a limited number of articles that contain studies of various resistors and resistor networks. Different articles on this topic have used different setups. Thus, carbon resistors exhibit the highest noise figure, followed by wirewound resistors [3], but significant differences can be observed in thin film resistors depending on the resistive material and the substrate of the resistor base. Excessive noise has been investigated in resistors [4], [5], and there is an understanding of its causes. It is possible to generalize the theoretical basis for noise in resistors [6]. In these studies, a method for noise characterization and the results of our own measurements performed on industrial resistors are presented. The most common in passive elements, in particular resistors, is thermal noise [7], [8]. It mainly affects the power spectrum and power spectral density of noise measured in an electrical circuit. In particular, one can consider how to calculate the thermal fluctuations of voltage/current on an equivalent Thevenin resistor, which can be measured at the output of a purely resistive circuit. There are other sources of noise that must be considered in any design to predict the impact of these noise sources on other parts of the circuit. This information can be used to model the noise [9], [10] in the time domain.

Testing and measuring the parameters of electronic components involves a number of different tasks, and one important task is noise analysis. In some cases, significant noise in a complex system can cause a device to fail, and it may not be obvious how the noise behaves just by looking at the signal in the time domain. Standard signal processing techniques are often represented in terms of continuous functions, but real-world measurements of electronic signals on measuring equipment are usually discretized. It is the noise power spectral density parameter that becomes an important tool for identifying and describing noise sources.

In this article, we propose an approach to measuring and analyzing the noise characteristics of industrial carbon resistors. The main attention is paid to the thermal type of resistor noise, which is the most typical and informative for resistive elements. Therefore, the noise characteristics measurements were carried out without an external load (without external power sources). Understanding and evaluating several resistor values is a motivation for research into other electronic devices.

II. Noise power analysis in electronics

A. Analysis of noise power spectral density in electronics

Noise quantities are usually expressed as the root mean square value of voltage or current, power spectral density (*PSD*), or amplitude spectral density (*ASD*). The power spectral density represents energy density per unit frequency interval with the unit A^2/*Hz* or V^2/*Hz*. When *PSD* is expressed as *(f)*, the relationship between *PSD* and the root mean square noise voltage (or current) is given by formula (1).

Noise power σ^2:

$$\sigma^2 = \int_{-\infty}^{\infty} S_{xx}(f)df . \qquad (1)$$

Mean square noise voltage [or current]:

$$\sigma = \sqrt{\int_{-\infty}^{\infty} S_{xx}(f)df} . \qquad (2)$$

Mean square (*Root mean square deviation - RMS*) the power for a continuous noise signal is obtained by integrating the *PSD* over an infinite frequency range.

The above integrals are generalized for any frequency range. But they are mostly evaluated for a specific frequency band, that is, the appropriate frequency range in which the circuit will operate. By taking the above results, dividing by the bandwidth, and taking the square root, we obtain the power spectral density level of the noise in terms of voltage and current fluctuations in the electrical circuit. In summary, there is no specific bandwidth for thermal noise; it depends on the bandwidth of the circuit in which the noise exists. The difference in nature *1/f* noise that usually appears with thermal noise will have its own power spectral density that dominates at low frequencies.

These time-domain signals are less useful than frequency-domain power spectra (power spectral densities). If time-domain noise measurement data is available, this signal can be converted into a power spectrum and power spectral density, which can be used to identify the dominant noise sources. In conducted electromagnetic interference (*EMI*) tests, significant peaks from all of these noise sources can also be observed, including

thermal noise, fractional noise, *1/f* noise, or other random sources.

The most common way to record discrete-time signals is in the time domain, as they are most commonly used in testing and measurement as well as in simulation. However, it is possible to transform discrete-time equations into integrals and use them for continuous signals. There are various ways to calculate the power spectral density for any discrete-time function [11], [12], [13].

The power spectral density for a discrete or continuous signal in the time domain obeys fairly simple relations. Calculation of the power spectral density for *N*-discrete signals with an interval *Δt*:

$$S(f) = \frac{1}{N}\left(\sum_{n=1}^{N} x(\Delta t) \cdot e^{-i2\pi f n \Delta t}\right)^2 . \qquad (3)$$

Thus, using the discrete Fourier transform, an arbitrary time-domain signal *x(t)* can be sampled at intervals of *Δt* seconds. The sampling window contains N samples and has a total time duration *T = NΔt.*

When using the autocorrelation parameter, we can use the Weiner-Hinchin theorem, which states that the autocorrelation function *x(t)* and the power spectral density are pairs of Fourier transforms [14]. Then we can represent *x(t)* as a function of the number of samples *n*. For a time-invariant noise source (stationary process), the power spectral density can be calculated using the following equation:

$$R(k) = \frac{1}{Var[x]}\sum_{n=1}^{N} x(n) \cdot x(n-k) , \qquad (4)$$

where *Var[x]* is the means the variance of a random variable *x*.

The power spectral density *S(f)* is the discrete Fourier transform of the autocorrelation function *R(k):*

$$S(f) = \sum_{k=1}^{N} R(k) \cdot e^{-i2\pi f k} . \qquad (5)$$

The presented autocorrelation process is also applicable to the determination of cross-power spectral density, where the cross correlation between two discrete signals is used to calculate the cross-power spectral density in the above equation.

B. Noise in resistors

The total signal of a device can be divided into the actual signal and the noise part. Therefore, the noise is characterized by its root mean square value. Intrinsic noise is noise that is generated within the system. The cause of this noise is the discrete nature of the charge carriers. The most relevant noise types for intrinsic noise are thermal noise, shot noise, burst noise, generation-recombination noise, excess noise (1/*f*-noise), and 1/f^2-noise [15], [16]. Noise types generally

have two main characteristics. The first is related to the physical phenomena that create the noise, and the second is their frequency distribution. Every measured signal contains some noise [17], [18], [19]. The voltage measured at the sensor output is equal to:

$$U(t) = U_{sig}(t) + U_n(t) , \qquad (6)$$

where U_{sig} is the actual voltage signal, and Un is the noise component of the voltage. Usually, the arithmetic mean is used to characterize the signal $\overline{U(t)}$. The arithmetic mean of noise is always zero. For the noise characteristic, it is customary to take the root mean square value, and it is given as:

$$U_{rms}(t) = \sqrt{U_n{}^2(t)} , \qquad (7)$$

which is used to quantify noise voltage.

Thermal noise. Thermal noise is the most common form of noise. It is also called Johnson noise, Johnson-Nyquist noise, or white noise. The main characteristic of thermal noise is its Gaussian amplitude distribution. The charge level fluctuations occur at the ends of each resistor. This time-dependent noise voltage is referred to as thermal noise. Thermal noise does not depend on the material or configuration of the electrical circuit, but only on constants. The noise density of the voltage of thermal noise, which is constant with respect to frequency, is given by:

$$U_{th} = \sqrt{4 k_B T R} , \qquad (8)$$

where U_{th} – is the effective thermal noise voltage in a given 1 Hz bandwidth, $k_B \approx 1{,}38 * 10^{-23} J/K$ – is the Boltzmann constant, T –is the absolute temperature in K, and R – is the resistance in *Ohms*. Similar to the definition of voltage noise density, the short-circuit noise density I_{th} is given by:

$$I_{th} = \sqrt{4 k_B T / R} . \qquad (9)$$

Thermal noise is always present in electronic circuits and is one of the main sources of noise. It becomes a signal integrity problem in low-level digital signals with low signal-to-noise ratio (*SNR*), i.e., high noise level. Thermal noise intensity and thermal noise bandwidth are also extremely important in radio frequency circuits.

Thermal noise will always occur in any component due to the inherent *DC* resistance of the system and has an autocorrelation function, which is a delta function. This means that thermal noise is not correlated in time; the thermal noise that is measured is independent of the thermal noise measured at all previous times. The bandwidth of thermal noise depends on the bandwidth of the circuit in which the noise is present. The root mean square (*RMS*) noise voltage and current across the impedance *Z* of the circuit can be calculated [7]:

$$\overline{U}_{rms}^2 = 4 k_B T \int_0^\infty \eta(f) \mathrm{Re}[Z(f)] df , \qquad (10)$$

$$\eta(f) = \frac{hf}{k_B T (e^{\frac{hf}{k_B T}} - 1)} , \qquad (11)$$

h - Planck's constant. These equations have an important consequence; the resistive part of the circuit determines the voltage associated with thermal noise. Because the rms voltage noise arises only through the resistive part of the circuit, the above integral can be written in terms of the Thevenin equivalent resistance, R_{th}. At sufficiently low frequencies, the coefficient η approaches unity and can be neglected. For a purely resistive circuit, the following result is:

$$Noise\,PSD = \sqrt{\left(\frac{\overline{U}_{rms}^2}{\Delta f}\right)} = 2 \sqrt{k_B T R_{th}} , \qquad (12)$$

where Δf is the thermal bandwidth, which is an arbitrary value chosen for a particular frequency range. Thermal noise in component specifications is usually expressed as the power spectral density (unit: V per square root of frequency) over a particular frequency range.

The *RMS* thermal noise current for an arbitrary input is determined in a similar way.

C. *Noise Spectrum Transformation and DFT/FFT*

The Discrete Fourier Transform (*DFT*) is used to transform a signal from the time domain to the frequency domain, which is the calculation of frequency components from time series data [20], [21]. The result of the transformation is the spectrum, or power spectral density *PSD* of the signal. *DFT* is a nonparametric method for estimating the spectrum, meaning it does not assume that the data fits a particular model and is a fairly robust method. Fast Fourier Transform *FFT* is a computationally efficient algorithm for computing the *DFT*. In practice, the two terms are often used interchangeably. *DFT* works by fitting sine and cosine waves of different frequencies to the time series data. The correlation between the sine and cosine waves of a particular frequency then gives the value of that frequency in the frequency spectrum.

Noise spectra are often displayed in a normalized format (*PSD*) or amplitude spectral density (*ASD*). This normalizes the data to a power spectrum (square of magnitude) or amplitude spectrum, which can be measured using an ideal bandpass filter with a bandwidth (bin) of 1.0 *Hz*. With a bin width (*Δf*), the spectrum is corrected for the *FFT* window used. The spectrum from the analyzer can be converted to a *PSD* using equation (13):

$$PSD = \frac{spectrum^2}{\Delta f \cdot NPB} , \qquad (13)$$

where *spectrum* represents the spectrum of the *FFT* value, *Δf* is the bin width, and *NPB* (*Noise Power Bandwidth*) is a correction factor for the *FFT* window used. The noise power bandwidth is compensated by the fact that the *FFT* window spreads the energy from the signal component at any discrete frequency to the neighboring elements. If the spectrum is given in units of *V* (volts), the *PSD* is given in units of *V²/Hz*. In the digital domain, for a spectrum in units of *FS*, the *PSD* will be in units of *FS²/Hz*. Then *ASD* is the square root of the power spectral density (Equation 14). Then ASD is the square root of the power spectral density (Equation 14):

$$ASD = \sqrt{PSD} = \frac{spectrum}{\sqrt{\Delta f \cdot NPB}} . \qquad (14)$$

For a spectrum in units of *V* or *FS*, it has units of *V/√Hz* or *FS/√Hz*, respectively.

The *rms* noise level in an arbitrary spectral passband can be determined by integrating the power spectral density over that frequency band. For the entire frequency band up to half the sampling frequency ($f_S/2$), the noise level is calculated by summing all *FFT* bins (as shown in equation 15):

$$U_{th} = \sqrt{\left(\sum_{i=1}^{NumBins} PSD_i \right) \cdot \Delta f} = \sqrt{\frac{\sum (Bin_i)^2}{NPB}} . \quad (15)$$

D. Frequency density and noise of a discrete representation

Thus, the calculation of the *DFT* requires several operations of order N^2. To facilitate the computational process, various algorithms have been developed, known under the abbreviation *FFT*, which reduce the number of operations to $N \times lnN$). *DFT/FFT* allows analyzing the frequency of various processes [22], [23]. Thus, there is a representation of the discrete Fourier transform, completed during the analysis of the frequency of the sampled signal. For example, in the simple case of an amplitude-modulated sinusoidal signal, after performing the sampled signal, it is possible to establish the presence of one frequency in the Fourier spectrum: the frequency of sinusoidal oscillations [24]. For more complex processes, a larger number of frequencies is expected [25].

The *FFT* function automatically imposes some restrictions on the time series that need to be estimated in order to produce a meaningful, accurate frequency response. Since the *FFT* function uses the base-2 logarithm by definition, it requires that the range or length of the time series to be estimated contain the total number of data points. It is exactly equal to the power of 2 (for example: 512, 1024, 2048, 4096, etc.). Therefore, the *FFT* can only estimate a fixed-length waveform containing 512, or 1024, or 2048, or 4096 points. The probability that the time domain contains a power of 2 numbers of points and ends with an integer number of periods is small at best.

Since the time domain under analysis is discretized in time, the frequencies must also be discretized. The domain *x(t)* is collected in a time window with *N* samples, and the value of f in the above equations is limited to the following set of *N* frequencies. The value of the n_{th} discrete frequency depends on the sampling frequency and is determined by:

$$f_1 = \frac{f_c}{N}, \quad f \in f_n, \quad f_n = \frac{n}{N} \cdot f_{samp.} \quad . \qquad (16)$$

If the units of domain spread are V, then the units of power spectral density are *V²/Hz*, and the units of power spectrum are V^2. Power spectral density is also reported in *W/Hz, dBm/Hz*, or other units related to *dB*. Similarly, the signal sampling may be less than the reciprocal of the passband of the measuring instrument. In this case, all data in the power spectral density plot above the passband should be ignored.

III.   NOISE POWER SPECTRAL DENSITY MEASUREMENT

A. Measuring noise on an oscilloscope channel

Noise measurement is related to small signal measurements and is based on time measurements such as period or duty cycle. This process is performed directly on the signals that are fed into the input channels of an oscilloscope. Estimating the bandwidth, such as thermal noise, and how noise interacts with various components can help you make some important decisions about the design of an electrical circuit. Noise tests can also be used when testing electronic circuits by connecting the inputs to the desired channel and observing the signals in the time and frequency domains. Noise processes actually occur in the time domain, and this is where all digital quantities are measured. Hardware such as oscilloscopes converts time domain measurements into frequency domain data.

The resulting measurements are plotted against time using a mathematical function called track or time. The track function is the input signal for subsequent noise measurements. The method is based on a resistor noise test system and describes the testing of a resistor to establish noise quality characteristics. It helps to select a suitable resistor when there are current and noise level requirements.

The equipment consists of several parts. The isolated resistor is ideally free of current noise. Low-noise carbon
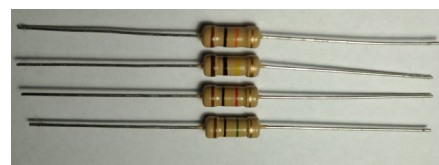

Fig. 1 Resistors for measuring thermal noise

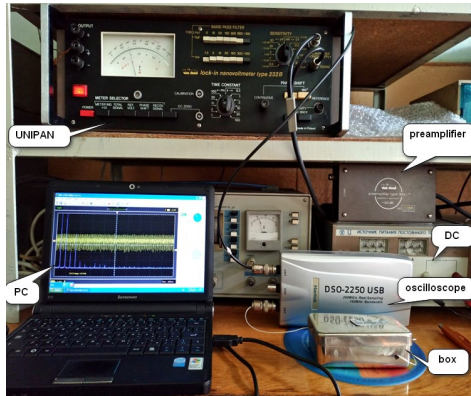resistors with standard values of 1 *kΩ*, 10 *kΩ*, 100 *kΩ* or

Fig. 2 Thermal noise measurement equipment

Fig. 3 Electrical circuit for measuring thermal noise

1 $M\Omega$ were used, resistor tests were performed in turn depending on the rating. An oscilloscope DSO-2250 with a fast Fourier transform (*FFT*) was used for recording. For voltmeters and similar data acquisition devices, the *FFT* should be performed later on a computer. By determining the *FFT* of the signal, it is possible to obtain information about noise in a wide frequency range. This provides more insight into the behavior of noise. In any case, the noise level of the measuring device should be taken into account.

The oscilloscope measures the *DC* voltage across the resistor under test and its noise (*PSD*). A constant load current was used. The voltage was measured using an instrumentation amplifier Unipan 232-B connected to the oscilloscope with a built-in *FFT* (Fig. 2). This makes the use of an amplifier mandatory for most installations. The next requirement for an amplifier in a noise measurement system is that the amplifier should produce as little noise as possible. Shielding is used because measuring excessive noise is a difficult task. The purpose of shielding is to protect against unwanted electromagnetic radiation from the outside.

Our research was aimed at identifying sources of fluctuations in industrial resistors of various nominal values in order to use oscilloscope-based equipment to calibrate thermal noise. Low-frequency noise was analyzed in the time and frequency domains, and excess noise associated with current flow was also investigated.

The Fig. 3 shows a general electrical circuit for researching the noise spectrum of electronic devices. The low-frequency noise measurement equipment consists of components, where R_x represents the measured resistor, R_f is the load resistance, and C_f is the capacitor shunting the *DC* voltage source (time constant $R_f \cdot C_f \approx 50$ s).

The thermal noise spectrum (Johnson-Nyquist) was measured with the *DC* power supply of the resistor under study turned off. In this case, there are no other noise mechanisms. The load resistance in our case was in the range 1$k\Omega \div$1 $M\Omega$. Also used is a signal low-noise voltage preamplifier 233-7 (20 dB) is a with a background noise spectral density of the order of 10^{-18} V^2 /Hz. The amplifier

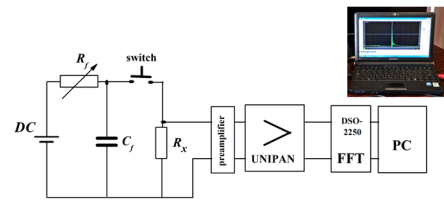connected to the closed-loop preamplifier demonstrated a total background noise spectral density of approximately 3x10^{-18} V^2 /Hz.

The preamplified signal (Fig. 4) is digitized (*A/D*), and the noise spectrum is performed in real time using a fast Fourier transform (*PC-FFT*). For frequencies below 200 *kHz*, thermal noise dominates (at all frequencies studied). 1/*f* noise components and explosive noise are not observed in the frequency range below 20 *kHz*. In this case, the *RMS* noise voltage of the resistor is proportional to the power.

To construct the noise power spectrum, we used the time domain of the noise signal taken from the test resistors. The signal was recorded on an oscilloscope through the amplification path. The gain on the oscilloscope was calibrated before the studies. The amplifier bandwidth was set within 1.5 *Hz*-150 *kHz*. Simultaneously (in parallel), the oscilloscope performed two measurements: the time domain of the amplitude and its *PSD* based on this domain. For the frequency domain, the built-in Blackman window was used. The frequency
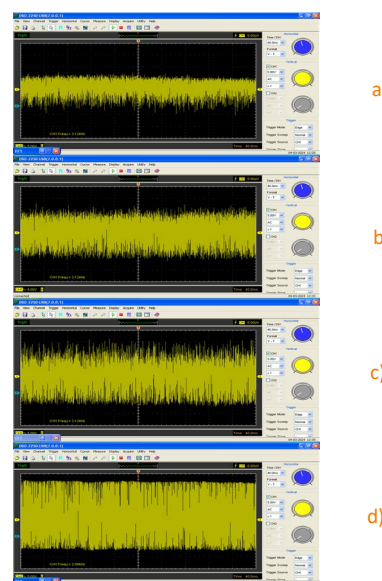

Fig. 4 Time domains of noise voltage for resistors with nominal values: a) – 1 kΩ, b) – 10 kΩ, c) – 100 kΩ, d) – 1 MΩ

window was set to the maximum sampling frequency using 4096 frequency bins. The frequency domain was recorded in *.xls* table mode. The conversion to a power spectrum (*PSD*) was performed by relating the square of the received voltage to the bandwidth of the measurement system. Typical *PSD* spectra obtained were presented graphically.

In parallel, the recorded time domains (*.xls* recording mode) of the measuring resistors were used to graphically present statistical information about thermal noise. This includes presenting histograms and estimating the standard deviation (as well as the variance) of the noise voltage. A detailed description of the properties of the measuring resistors based on the obtained noise characteristics is given below.

B. Analysis of time domain signals in the frequency domain

On an oscilloscope with an *FFT* (or dynamic signal analyzer), a marker is activated to measure noise, which is related to the magnitude of the noise voltage. Thus, noise is measured in rms units of volts. Noise is usually expressed in *nV/rt-Hz* (nanovolts per root hertz of the bandwidth). Instead of bandpass and resolution filters, the *FFT* analyzer has window functions, and these functions also have *ENBW*. The sampling rate and *FFT* size determine the *FFT* bin width.

DSOs are now quite common, and most of them have built-in *FFT* functions but do not have a "Noise Marker" function. The main reason is that they do not have very low noise. A basic DSO only needs 8 bits of vertical resolution to provide a very accurate signal trace. Therefore, the smallest possible analog bandwidth is used, for example, a built-in 200 *MHz* bandwidth limiter. To obtain data, you need to specify the digitizer sampling rate (F_s) and the data to use for the *FFT*. The *FFT* bin width is defined as:

$$\text{hopper width FFT} = F_s / \text{size FFT} . \qquad (17)$$

If the sampling rate is 200 *MHz* and the *FFT* size is 4096 data points, the resulting bandwidth is 48 *kHz*. The *FFT* size is the length of the input data to the *FFT* function or the length of the time domain record used. The actual data suitable for the *FFT* is half the size of the input data.

The value of spectral analysis lies in the ability to identify the spectral "*fingerprint*" of repetitive signals with frequencies that fall between the fundamental (1/ *data acquisition buffer*) and the Nyquist frequency (½ *sampling frequency*) [26], [27], [28].

To identify the source of noise, the oscilloscope automatically runs a Fast Fourier Transform almost in real time. The infinite addition of a signal creates a periodic waveform. When a waveform in the time domain is converted to the frequency domain, the result is a set of sine waves, each with a frequency, amplitude, and phase. In the time domain, the measurement is described by the total acquisition time – τ, and the time interval between samples – $\triangle t$. In the frequency domain, the spectrum is the collection of all the components of the sine wave — each with a frequency, amplitude, and phase. For a repeating waveform, the power of the *DFT* can be applied to mathematically calculate each frequency component in the spectrum [29].

The measurements for this experiment were made using an oscilloscope with a built-in *FFT* function. This device has a number of capabilities. The analyzer creates a spectrum – a graph of voltage versus frequency – by recording a sequence of voltage measurements (like a digital oscilloscope) and then performing a fast Fourier transform of the measurements (hence the initials "*FFT*"). The results of the Fourier transform are used in a variety of ways. For this experiment, two of these functions are used to obtain the noise voltage:

Spectrum averaging. Since the noise of interest is random over a wide frequency range, successive *FFT* spectra show deviations from one spectrum to the next. The processing technique allows for averaging successive spectra to reduce these deviations. To do this, the averaging function can be set to do an "exponential" rms averaging, for example, of 10 spectra.

Bandwidth analysis. In *FFT* analysis, the frequency axis, or "span," is divided into, for example, 400 equal intervals called "bins." For a full-width spectrum of 200 *kHz*, each bin represents an interval of 500 *Hz*; if the span is narrowed, each bin is narrowed accordingly. Bandwidth analysis combines measurements in adjacent regions to obtain the average voltage over a frequency interval greater than the width of one bin.

The appearance and noise spectrum for a 100 *kΩ* resistor are shown in Fig. 5. The traces show the total noise of the resistor U_{tot}. Oscillogram (bottom curve) illustrates the noise power spectral density for electronic components, starting at a frequency of $f_{min}=1/t_{meas}$
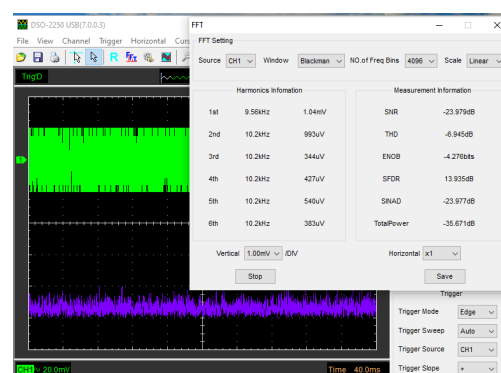

Fig. 5 Oscillogram of noise measurement of a 100 kΩ resistor: upper curve (green) – time domain, lower curve (violet) – FFT trans-formation
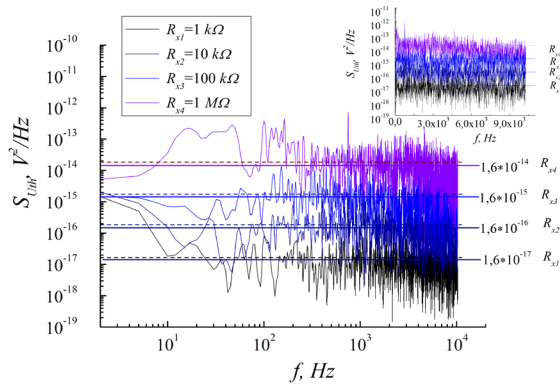
Fig. 6 Spectral dependences of noise power for different resistor values in logarithmic coordinates; horizontal lines − calculated values of thermal noise (inset – dependences in semi-logarithmic coordinates)

$(1/t_{meas}$ − time domain duration). The maximum frequency is determined by the time discreteness unit $f_{max}=1/\Delta t$. The noise density of the resistor is distributed over frequency. In this measurement, a resistance of $R=100\ k\Omega$ and an ambient temperature of $T = 25°C$ were assumed (we chose a typical resistor). From the noise voltage measured on the load resistor R_x, the spectral density S_U is calculated. The dependence of the spectral density of the voltage noise S_U on the frequency for a resistor at a temperature of $T = 25°C$ is shown in Fig. 6. The spectral density of the voltage noise is given by the superposition of noises. For thermal noise, the spectral density $S_{Uth} = 1{,}6\cdot10^{-15}\ V^2\ /Hz$.

When taking into account the excess current noise that can appear at low frequencies, a component of the power spectral density arises that varies inversely with frequency. The current noise voltage in a 1 Hz window has a value of $u_f = C\ /\ \sqrt{f}$. The constant C for a particular resistor can be obtained by measurements. The total noise voltage in the measurement range can be expressed in terms of the excess and thermal noise components:

$$U_n = \sqrt{U_f^2 + U_{th}^2}\ .\qquad(18)$$

The value of the measured noise voltage corresponds to formula (8). At room temperatures (approximate $k_B T \gg h\cdot f$), this noise voltage is determined by formula (12). Thermal noise is approximately white, meaning that its power spectral density is nearly equal throughout the frequency spectrum.

Using (18), we can describe the total noise in terms of its thermal component. The area under the total noise density curve for any given bandwidth f_1 to f_2 is the root mean square noise voltage. The parameter C can be described by the integral of the square of the voltage in equation (19) over the frequency range f_1 to f_2 [1], [6]:

$$U_n = U_{th} \cdot \sqrt{f_c \cdot \ln\frac{f_2}{f_1} + f_2 - f_1}\ .\qquad(19)$$

The lowest frequency component f_c is fundamental to the thermal noise and has a frequency content at which its magnitude is equal to the excess noise. This is the lowest- frequency sinusoid that can be accommodated in the acquisition time. The period P of this lowest frequency sinusoid is the total acquisition time τ. This means that the frequency interval between the resolutions is the fundamental frequency. The highest frequency component in the spectrum is related to the time interval between the sample points. This means that the period of the highest frequency sinusoid that can be calculated is twice the time interval. Since the sampling rate for acquiring the data is $1/\Delta t$, the Nyquist frequency, the highest frequency for which we can calculate the component, is half the sampling rate. To obtain higher resolution and to distinguish between closely spaced frequency features in the spectrum, it is necessary to use a longer acquisition time in the oscilloscope.

The *FFT* speed calculation is done by reducing the buffer to 2^n sample points. The *FFT* calculates the same integrals as the *DFT* but uses matrix mathematics to perform the calculations using a total number of points that is a power of 2. If there are five thousand points in buffer one, the largest number of points that can be included in the *FFT* calculation is $2^{12} = 4096$ points. The first step in performing the *FFT* is to determine the area of the acquisition buffer that contains the largest number of 2^n points that are being calculated. Most oscilloscopes allow you to select either the center area of the time domain screen or the left edge of the screen.

In the windowed approach, a periodically irregular signal processed by the *FFT* will have a smooth transition at the endpoints, resulting in a more accurate representation of the power spectrum. Each of the windows has different characteristics that make one window better than the others in separating spectral components that are close to each other in frequency.

The Blackman window offers a weighting function similar to the other windows but is characterized by a narrower shape, and due to its narrow shape, this window best represents the spectral domain.

The *PSD* parameter, power per unit frequency, is the most common frequency domain tool for noise analysis. The *PSD* is given in units of V^2/Hz. The trace is calculated using the oscilloscope's Fast Fourier Transform (*FFT*), choosing the output signal magnitude in squared units instead of the standard decibel (*dBm*) scale. The *FFT* setting sets the resolution bandwidth Δf, which in this case is 100 *kHz*, and the effective noise bandwidth (*ENBW*) of the weighting function, which is 1000 for rectangular weighting. In addition to reading the selected parameter for a particular acquisition, the oscilloscope
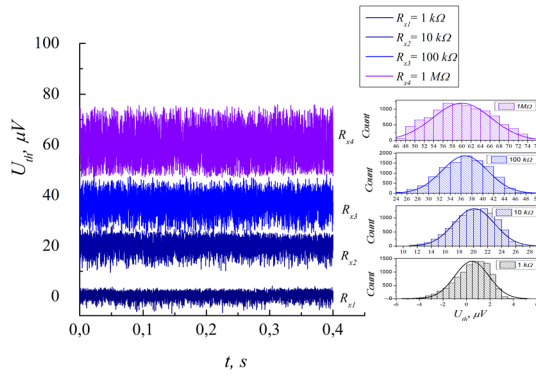
Fig. 7 Time domain noise for different resistor values (for clarity, these dependencies are shifted vertically). Inset shows corresponding histograms of dependencies

TABLE 1 ESTIMATES FOR RESISTORS OF DIFFERENT RATINGS

N	R_x, Ohm	PSD_{mean}/W_x, arb.units	$\delta(PSD_{mean}/W_x)$, %	δR_x, %
1	10^3	1,04	4	± 5
2	10^4	1,16	16	± 5
3	10^5	1,09	9	± 5
4	10^6	1,14	14	± 5

can calculate and display aggregate statistics for multiple acquisitions for each parameter, providing the average, maximum, minimum, and standard deviation for each parameter (fig. 7). The amplitude of the signal has very nearly a Gaussian probability density function. The Gaussian distribution is symmetric about the mean, with the probability of the amplitude value falling as the amplitude moves away from the mean. Extreme amplitudes (so-called tails) have a very low but non-zero probability of occurrence (Fig. 7-inset). The value of σ, which is included in the theoretical formula (2), allows us to judge the magnitude of the noise signal.

The *FFT* spectrum is a complex function (in the mathematical sense), and the magnitude representation is only half the picture. The *FFT* output consists of a real and imaginary part. Some oscilloscopes can display both. As an alternative to real and imaginary components, many oscilloscopes display the *FFT* phase along with the magnitude. These two paired output formats (*real/imaginary* and *magnitude/phase*) represent the complete *FFT* picture. The real/imaginary components are needed to calculate the inverse *FFT*. The magnitude/phase format is quite common in electrical measurements.

The characteristics of the spectral dependences of noise were estimated by the ratio of the average value of the thermal noise power spectral density (*PSD*) in the frequency range of measurements (white noise Johnson-Nyquist) and its calculated theoretical value by the ohmic rating of the measuring resistor. Estimates for resistors of different ratings are given in Table 1. The third column of the table indicates the ratio PSD_{mean}/W_x (thermal noise power $W_x = 4kTR_x$). The fourth and fifth columns are, respectively, the relative errors of the deviation of this ratio and the resistor value.

We also note that for measurements of a group of specific resistors, the ratio of their noise resistance to ohmic resistance does not deviate much from unity. This

indicates that their ohmic characteristics are approaching ideal. Noise resistance (which is included in the Nyquist equation) can also be determined by the magnitude of the *PSD* value of the calibrated system.

The possibilities of using noise measurements to assess the quality of thick-film resistors and to assess the degradation of their parameters under load have not been sufficiently investigated. The reason for this is the complexity of the microstructure of thick-film resistors and conduction mechanisms, as well as the insufficient understanding of their relationship with noise. Taking into account the current trend of miniaturization and mass use in modern highly sensitive communication systems, little attention has been paid to the influence of, for example, impulse loads on the structure and noise characteristics of conventional thick-film resistors. It has been shown [30] that low-frequency noise, expressed in terms of noise index or resistance noise spectrum, is more sensitive to resistor degradation caused by impulse loads than resistance. The quality assessment of thick-film resistors and the analysis of degradation processes can be performed based on measurements of resistance and noise index using and transport characteristics. It is as an indicator of quality and degradation for thick-film resistors.

Theoretical developments of the model of low-frequency noise in film resistors were developed by the authors [31]. This model is based on the phenomena of fluctuations in electron capture by traps during electron transport through insulating layers and on tunneling processes. In particular, this model is applied to thick-film structures. The specified fluctuation mechanism can affect the level and shape of the noise spectrum. Thick-film resistors are complex systems. The parameters of low-frequency noise are sensitive to the structure of the thick film, and noise measurements can be used as a tool for analyzing the quality of a film resistor.

When the microstructure of the resistive material is disrupted, the noise intensity is higher. Moreover, there can be a catastrophic increase in noise by several times [32], while the additional resistance will increase by only a few percent. In [5], a model of excess resistor noise is proposed, which includes the effect of current accumulation around multipoint contacts. It is shown that such accumulation has a much greater effect on the noise of the device under study than on its resistive resistance. It

is proposed to use noise as a diagnostic tool for assessing the quality and reliability of electronic devices.

These results can also be used to calculate the noise figure of a low-noise amplifier in the frequency range under study [33]. The noise figure *NF* is defined as:

$$NF = 20\log 10 \frac{U_{measured}}{\sqrt{2k_B TR \cdot NPB}} [dB] . \qquad (20)$$

It is the difference in decibels between the noise of a real amplifier with a certain input resistance *R* and an ideal noiseless amplifier with the same input resistance.

CONCLUSION

The work quantifies random processes such as noise using time, frequency, and statistical processing tools, supplemented by appropriate measurement parameters using a digital oscilloscope. The main statistical parameters, including the mean, standard deviation, and measurement range, provide an idea of the measured noise characteristics process. A spectral analysis has been developed to identify the spectral time signature in the frequency range between the fundamental (1/*data acquisition buffer*) and Nyquist frequency (½ *sampling frequency*). To identify noise sources, a fast Fourier transform of the signal in real time on an oscilloscope has been launched. The *FFT* tool has been used to determine the thermal (white) noise spectra using the total number of points in the *FFT* calculation of $2^{12} = 4096$ points for industrial resistors of various nominal values.

There are specific features that characterize a certain type of noise. In this case, thermal noise dominates in measuring elements (a group of industrial resistors) — three features are given, in particular, this is the proportionality of the noise voltage to the root of the resistive resistance, the noise is "white" and has a normal statistical distribution (Gaussian shape). The deviation from the ideality of the resistor by thermal noise is estimated by the ratio of the noise resistance to the resistive (where the actual noise resistance of the resistor is determined from the value of the thermal noise - *PSD*).

Thermal noise measurement techniques can be used to diagnose resistors (and other electronic devices) in laboratory environments. For measurements of a group of specific resistors, the ratio of their noise resistance to ohmic resistance does not significantly deviate from unity. However, it is difficult to give any recommendations on which setup should be used for specific types of resistors. This is due to the different resistor manufacturing technologies (carbon composition, wire wound, thin film, metal film resistors). For most publications on electronic noise measurements, only a few measurement results are available.

REFERENCES

[1] D. Walter, A. Bülau, A. Zimmermann "Review on Excess Noise Measurements of Resistors", Sensors, vol.1107, no 3, pp.1-29, 2023, **DOI:** 10.3390/s23031107.

[2] M. M. Jevtic, I. Mrak , Z. Stanimirovic "Thick-film resistor quality indicator based on noise index measurements", Microelectronics Journal, vol. 30, no.12, pp. 1255–1259, 1999, **DOI:** 10.1016/S0026-2692(99)00050-6.

[3] D. Rocak, D. Belavic, M. Hrovat, J. Sikula, P. Koktavy, J. Pavelka, V. Sedlakova "Low-frequency noise of thick-film resistors as quality and reliability indicator", Microelectronics Reliability, vol. 41, no. 4, pp. 531-542, 2001, **DOI:** 10.1016/S0026-2714(00)00255-9.

[4] M. M. Jevtic, Z. Stanimirovic, I. Stanimirovic "Evaluation of thick-film resistor structural parameters based on noise index measurements", Microelectronics Reliability, vol. 41, no.1, pp. 59-66, 2001, **DOI:** 10.1016/S0026-2714(00)00207-9.

[5] E. P. Vandamme, L. K. J. Vandamme "Current crowding and its efect on 1/f noise and third harmonic distortion a case study for quality assessment of resistors", Microelectronics Reliability, vol. 40, no. 11, pp. 1847-1853, 2000, **DOI:** 10.1016/S0026-2714(00)00091-3.

[6] L. Chen, Y. Duan, Y. Liang "Analysis of non-ideal factors for a high precision interpolated resistor string DAC", Microelectronics Journal, vol. 143, no. 106049, pp. 1-6, 2024, **DOI:** 10.1016/j.mejo.2023.106049.

[7] L. B. Kish "Zero-point thermal noise in resistors? a conclusion", Metrol. Meas. Syst., vol. 26, no. 1, pp. 3–11, 2019, **DOI:** 10.24425/mms.2019.126337.

[8] R. Tavcar, J. Bojkovski, S. Begus "Sound-card-based Johnson noise thermometer", Measurement, vol. 225, no. 114077, pp. 1-6, 2024, **DOI:** 10.1016/j.measurement.2023.114077.

[9] A. Ghosh "Generalised energy equipartition in electrical circuits", Pramana – J. Phys., vol. 97, no. 82, pp.1-6, 2023, **DOI:** 10.1007/s12043-023-02553-w.

[10] I. S. Virt, I. S. Bilyk, O. A. Parfeniuk, M. I. Ilashchuk "Noise and transport properties of CdTe <Pb> crystals", Microsystems, Electronics and Acoustics, vol. 17, no. 4, pp. 5-10, 2012, **DOI:** 10.20535/2312-1807.2012.17.4.218982.

[11] J. Kim, J. Kim, C. D. de Souza "Discrete time domain analysis of radiation detector noise", Nuclear Inst. and Methods in Physics Research A, vol. 1021, no. 165925, pp. 1-14, 2022, **DOI:** 10.1016/j.nima.2021.165925.

[12] O. M. Adegoke, I. B. Oluwafemi, O. Akinsanmi "A Time Domain Noise Measurement and Analysis for Broadband Indoor Power Line Communications", Instrumentation Mesure Metrologie, vol. 19, no. 2, pp. 103-110, 2020, **DOI:** 10.18280/i2m.190204.

[13] Z. Sita, V. Sedlakova, J. Majzner, P. Sedlak, J. Sikula , L. Grmela "Analysis of noise and non-inearity of I-V characteristics of positive temperature coefficient chip thermistors", Metrol. Meas. Syst., vol. 20, no. 4, pp. 635–644, 2013, **DOI:** 10.2478/mms-2013-0054.

[14] G. T. Seidler and S. A. Solin "Non-Gaussian 1/f noise: Experimental optimization and separation of high-order amplitude and phase correlations", Physical Review B, vol. 53, no. 15, pp. 9753- 9759, 1996, **DOI:** 10.1063/1.2759716.

[15] K. Mleczko, Z. Zawislak, A.W. Stadler, A. Kolek, A. Dziedzic, J. Cichosz "Evaluation of conductive-to-resistive layers interaction in thick-film resistors", Microelectronics Reliability, vol. 48, no. 6, pp. 881–885, 2008, **DOI:** 10.1016/j.microrel.2008.03.012.

[16] A.W. Stadler "Noise properties of thick-film resistors in extended temperature range", Microelectronics Reliability, vol. 51, no. 7, pp. 1264-1270, 2011, **DOI:** 10.1016/j.microrel.2011.02.023.

[17] Z. Balogh, G. Mezei, L. Pósa, B. Santa, A. Magyarkuti and A. Halbritter "1/f noise spectroscopy and noise tailoring of nanoelectronic devices", Nano Futures, vol. 5, no. 4, p.1-11, 2021, **DOI:** 10.1088/2399-1984/ac14c8.

[18] E. J. McDowell, X. Cui, Z. Yaqoob, and C. Yang "A generalized noise variance analysis model and its application to the characterization of 1/f noise", Optics Express, vol. 15, no. 7, pp. 3833-3848, 2007, **DOI:** 10.1364/oe.15.003833.

[19] S. Demolder, M. Vandendriessche, and A. Van Calster "The measuring of l/f noise of thick and thin film resistors", Journal of Physics E Scientific Instruments, vol. 13, no. 12, pp. 1323-1327, 2000, **DOI:** 10.1088/0022-3735/13/12/024.

[20] B. Stawarz–Graczyk, A. Szewczyk, and A. Konczakowska "Identification of inherent noise components of semiconductor devices on an example of optocouplers", Opto–Electronics Review, vol. 17, no. 3, pp. 236–241, 2009, **DOI:** 10.2478/s11772-008-0073-5.

[21] P. Sakalas, A. Šimukovič, S. Piotrowicz, O. Jardel, S. L. Delage, A. Mukherjee, A. Matulionis "Compact modelling of InAlN/GaN HEMT for low noise applications", Semicond. Sci. Technol., vol. 29, no. 9, pp. 1- 8, 2014, **DOI:** 10.1088/0268-1242/29/9/09501.

[22] M.S. Priyadarshini, M. Bajaj, L. Prokop, M. Berhanu "Perception of power quality disturbances using Fourier, Short Time Fourier, continuous and discrete wavelet transforms", Scientifc Reports, vol. 14, no.1, pp. 1-40, 2024, **DOI:** 10.1038/s41598-024-53792-9.

[23] Y. Tong, L. Wang, W.-Z. Zhang, M.-D. Zhu, X. Qin, M. Jiang, X. Rong, and J. Du "A high performance fast-Fourier-transform spectrum analyzer for measuring spin noise spectrums", Chin. Phys. B, vol. 29, no. 9, pp. 1-8, 2020, **DOI:** 10.1088/1674-1056/ab9c04.

[24] K. R. Rao, D. N. Kim, J. J. Hwang "Fast Fourier Transform: Algorithms and Applications", Springer Dordrecht Heidelberg, London New York Library of Congress # Springer Science, 2010, **DOI:** 10.1007/978-1-4020-6629-0.

[25] U. Meyer-Base, H. Natarajan, A. G. Dempster "Fast Discrete Fourier Transform Computations Using the Reduced Adder Graph Technique", Eurasip Journal on Advances in Signal Processing, vol. ID 67360, pp. 1-8, 2007, **DOI:** 10.1155/2007/67360.

[26] K. Sozanski "Overview of Signal Processing Problems in Power Electronic Control Circuits", Energies, vol. 16, no. 4774. pp.1-26, 2023, **DOI:** 10.3390/en16124774.

[27] E. Serrano-Finetti, O. Casas, R. P. Areny "Common mode electronic noise in differential circuits", Measurement, vol. 140, no.7, pp. 207-214, 2019, **DOI:** 10.1016/j.measurement.2019.04.028.

[28] P. Ashdhir, J. Arya, C. E. Rani and A. Eur "Exploring the fundamentals of fast Fourier transform technique and its elementary applications in physics", J. Phys., vol. 42, no. 065805, pp. 1- 28, 2021, **DOI:** 10.1088/1361-6404/ac20ad.

[29] M. A. Ogunlade, S. L. Gbadamosi, I. E. Owolabi, N. I. Nwulu "Noise Measurement, Characterization, and Modeling for Broadband Indoor Power Communication System: A Comprehensive Survey ", Energies, vol. 16, no. 1535, 2023, pp. 1-26, **DOI:** 10.3390/en16031535.

[30] I. Stanimirovic, M.M. Jevtic, Z. Stanimirovic "High-voltage pulse stressing of thick-film resistors and noise", Microelectronics Reliability, vol. 38, no. 10, pp. 1569-1576, 1998, **DOI:** 10.1016/S0026-2714(98)00032-8.

[31] I. Mrak, M.M. Jevtic, Z. Stanimirovic "Low-frequency noise in thick-film structures caused by traps in glass barriers", Microelectronics Reliability, vol. 38, no. 10, pp. 1569-1576, 1998, **DOI:** 10.1016/S0026-2714(98)00032-8.

[32] L.K.J. Vandamme, A.J. Van Kemenade "Resistance noise measurement: A better diagnostic tool to detect stress and current induced degradation", Microelectronics Reliability, vol. 37, no. 1, pp. 87-93, 1997, **DOI:** 10.1016/0026-2714(96)00241-7.

[33] T.-Y. Lin, R.J. Green, P.B. O'Connor "A low noise single-transistor transimpedance preamplifier for Fourier-transform mass spectrometry using a T feedback network", Rev. Sci. Instrum. vol. 83, no. 094102, pp. 1-7, 2012, **DOI:** 10.1063/1.4751851.

Вимірювання шумів у електронних пристроях методом Фур'є перетворення

І. В. Падалка[f], 🔵 0009-0007-4071-5878

І.С. Вірт[s], д-р фіз.-мат. наук проф., 🔵 0000-0001-7200-6055

Дрогобицький державний педагогічний університет імені Івана Франка ℝ 04vpyax58
Дрогобич, Україна

Анотація—У роботі розглянуто та проаналізовано метод вимірювання шумових характеристик електронних кіл та пристроїв на основі збору даних цифровим осцилографом з вбудованим Фур'є перетворенням. Методика процесу вимірювань та її аналіз продемонстровані на визначенні шумових характеристик промислових резисторів. Це, зокрема, термічного (білого) шуму у який є переважаючим типом шуму для резисторів. Робота містить огляд шумових властивостей резисторів, існуючих методів вимірювань, а також питань теорії таких вимірювань.

Для визначення джерел шуму у промислових резисторах запущено швидке перетворення Фур'є сигналу (*FFT*) в реальному часі на осцилографі. Засобом *FFT* визначено спектри теплового (білого) шуму використовуючи загальну кількість точок 2^{12}. Тим не менш, важко дати будь-які рекомендації щодо того, яке устакування слід використовувати для певного типу або технології резистора, оскільки для більшості установок рівень шуму невідомий і доступні лише деякі результати вимірювань.

Оцінено відношення середнього значення спектральної густини потужності теплового шуму (PSD) в частотному діапазоні вимірювань до його розрахункового теоретичного значення за омічним номіналом вимірювальних вугільних промислових резисторів.

Ключові слова — електронні пристрої; резистори; спектральний аналіз; перетворення Фур'є; термічний шум; шумова діагностика.